Nucl. Phys. B 1028 (2026) 117511

Contents lists available at ScienceDirect

Nuclear Physics, Section B

journal homepage: www.elsevier.com/locate/nuclphysb

Quantum Field Theory and Statistical Systems

Monte Carlo studies of the two-dimensional XY model with four-fold anisotropy

Truong Thi Bach Yen [a,b], Le Thi Thao Vien [c], Nguyen Tri Tuan [a], Dinh Manh Tien [a], Nguyen Duc Dung [d], Hoang Mai Anh [d], Tran Truong Giang [d], Nguyen Vo Nguyen Huy [d], Le Chi Luan [e], Duong Xuan Nui [e], Dao Xuan Viet [d,*]

[a] College of Natural Sciences, Can Tho University, Can Tho, Vietnam
[b] Faculty of Natural Sciences Teacher Education, Dong Thap University, Dong Thap, Vietnam
[c] Faculty of Natural Sciences, Quy Nhon University, Quy Nhon, Vietnam
[d] School of Materials Science and Engineering, Hanoi University of Science and Technology, Hanoi, Vietnam
[e] Faculty of Information Technology, University of Transport Technology, Hanoi, Vietnam

ARTICLE INFO

Editor: Shuang Wu

Keywords:
Phase transitions
Monte Carlo method
2D XY model
Anisotropy

ABSTRACT

Early theoretical studies of the two-dimensional XY model with four-fold anisotropy (XYh_4) predicted that any finite anisotropy should completely suppress Kosterlitz–Thouless (KT) transition of the isotropic system and replace it with a second-order phase transition. This prediction is inconsistent with Monte Carlo (MC) simulations, which suggested KT-like behavior at weak anisotropy. To resolve this discrepancy, we performed large-scale MC simulations to systematically examine the XYh_4 model across a wide range of anisotropic strengths. Our results indicate that while weak anisotropy can mimic KT behavior in small systems, a detailed finite-size scaling analysis of larger systems reveals that the temperature derivative of Binder ratio and the correlation length ratio displays scaling behaviors characteristic of a second-order transition even at the weak h_4 values. The critical exponent ν is non-universal and varies continuously with h_4 from weak to strong anisotropy. These findings confirm that XYh_4 model exhibits a second-order phase transition for weak finite anisotropy, effectively reconciling theoretical predictions with numerical observations.

1. Introduction

The two-dimensional (2D) planar rotator model, commonly known as the XY model, is a fundamental system in statistical physics that exhibits unique properties despite the simplified nature of its two-component spins. A particularly notable feature is the presence of a low-temperature Kosterlitz-Thouless (KT) phase. The KT phase is instead characterized by an algebraic decay of correlation functions, leading to a divergent susceptibility. The transition from the KT phase to the high-temperature paramagnetic phase at a critical temperature T_c is suggested to involve an essential singularity in the correlation length, distinguishing it from the algebraic singularity seen in the Ising model transition.

* Corresponding author.
E-mail address: viet.daoxuan@hust.edu.vn (D.X. Viet).

https://doi.org/10.1016/j.nuclphysb.2026.117511
Received 9 December 2025; Received in revised form 9 May 2026; Accepted 13 May 2026
Available online 15 May 2026

Introducing a symmetry-breaking field, commonly referred to as crystal-field anisotropy, is a standard approach for modeling realistic materials and examining the stability of the KT phase. Early theoretical studies based on renormalization-group (RG) analysis [1–3] predicted that for $p = 4$ the system should exhibit only a single order–disorder phase transition. This transition is expected to be continuous, with non-universal critical exponents depending on the strength of the anisotropy field. Within this framework, the KT phase characteristic of the isotropic case ($h_4 = 0$) is predicted to be suppressed for any finite fourfold anisotropy ($h_4 \neq 0$). In the limit of very strong anisotropy, the model reduces to the four-state clock model, which is equivalent to two decoupled Ising models and therefore exhibits a single phase transition in the Ising universality class.

However, experimental measurements and extensive Monte Carlo (MC) simulations have revealed a more nuanced picture [4,5]. Although intermediate and strong h_4 fields indeed lead to transitions with nonuniversal exponents, experimental data often fall within a "universal window" bounded by the Ising ($\beta \approx 0.125$) and XY ($\tilde{\beta} \approx 0.23$) values, contrary to the theoretical prediction of a potentially divergent exponent. Furthermore, MC simulations [6,7] for weak h_4 evidence of a pocket of XY behavior at intermediate temperatures, characterized by $\tilde{\beta} \approx 0.23$, similar to the $p > 4$ cases. This suggests that the KT phase persists for finite, albeit weak, h_4, with the transition scenario crossing over to the non-universal XYh_4 behavior as h_4 increases. The robustness of the KT phase in the thermodynamic limit for weak h_4 remains an open question [5].

To further investigate the discrepancy between theoretical predictions and numerical observations on the stability of the KT phase for the XYh$_4$ model, we have conducted extensive MC simulations. Our simulations were performed on the square planar rotator model with varying strengths of the four-fold anisotropy $0.001 \leq h_4 \leq 5$, which spans from a weak to a strong anisotropy. We measure several physical quantities, including the specific heat, the susceptibility, the Binder ratio, the temperature derivative of the Binder ratio, the correlation length ratio, and the Z_4 symmetric magnetization. Our numerical findings suggest that the system undergoes a second-order phase transition from strong to weak anisotropy. The $T - h_4$ phase diagram of the 2D XYh_4 model is also established.

2. Model and methods

The Hamiltonian of this model is given as follows [1]:

$$H = -J \sum_{\langle ij \rangle} \cos(\theta_i - \theta_j) - h_4 \sum_i \cos 4\theta_i, \tag{1}$$

where θ_i presents the angle of spin i relative to the x-axis, taking values within the range $[0 : 2\pi]$. J represents the nearest-neighbor exchange interaction. The symbol $\langle ij \rangle$ indicates that the sum is taken over the nearest-neighbor lattice sites. The first term describes the exchange interaction between neighboring spins, while the second term represents the four-fold crystal-field anisotropy acting on each spin. In this work, we use dimensionless units setting $J = 1$ and Boltzmann constant $k_B = 1$.

MC simulations are performed for the two-dimensional XYh_4 model in a square lattice with periodic boundary conditions. For each temperature, the system is initialized with a random spin configuration. The update scheme combines the Metropolis algorithm for local single-spin updates and the embedded Wolff algorithm for cluster updates [8–12]. One MC step consists of a Metropolis sweep followed by an embedded Wolff sweep, described as follows:

(1) Choice of the reflection axis: A random unit vector $\mathbf{r}$ is chosen as the reflection axis.

(2) Projection of spins: Each spin $\mathbf{S}_i = (\cos\theta_i, \sin\theta_i)$ is projected onto this axis, giving $\sigma_i = \mathbf{S}_i \cdot \mathbf{r}$

(3) Cluster seed: A lattice site i is randomly chosen as the initial site of the cluster. Its spin is reflected about the axis $\mathbf{r}$: $\mathbf{S}_i \to \mathbf{S}_i' = \mathbf{S}_i - 2(\mathbf{S}_i \cdot \mathbf{r})\mathbf{r}$

(4) Cluster growth: For each neighbor j of a site i already in the cluster, site j is added to the cluster with probability $P_{ij} = 1 - \exp\left[-2J(\sigma_i\sigma_j)/(k_BT)\right]$. This process continues until no additional sites are added.

(5) Embedded anisotropy: The anisotropic energy change associated with the reflection is calculated as $\Delta E_{\text{anis}} = \sum_{i \in Cluster} \left[h_4\left(\cos(4\theta_i') - \cos(4\theta_i)\right)\right]$.

(6) Cluster flip: The cluster update is accepted with Metropolis probability $P_{\text{accept}} = \min\left(1, e^{-\Delta E_{\text{anis}}/(k_BT)}\right)$. If accepted, all spins in the cluster are reflected across the axis $\mathbf{r}$.

The embedded Wolff algorithm satisfies a detailed balance as follows. Denoting by $T(S \to S')$ the probability of generating the embedded-cluster move from configuration S to S', the transition probability is

$$W(S \to S') = T(S \to S')\min[1, e^{-\beta\Delta E_{\text{anis}}}]. \tag{2}$$

Since the Wolff embedded-cluster construction satisfies detailed balance for the isotropic part of the Hamiltonian,

$$e^{-\beta E_{\text{iso}}(S)}T(S \to S') = e^{-\beta E_{\text{iso}}(S')}T(S' \to S). \tag{3}$$

Multiplying both sides by the Metropolis factor for the anisotropy term gives

$$e^{-\beta E(S)}W(S \to S') = e^{-\beta E(S')}W(S' \to S), \tag{4}$$

where $E = E_{\text{iso}} + E_{\text{anis}}$. Therefore, detailed balance holds for the full Hamiltonian.

The simulation parameters for $h_4 = 1$ and $h_4 = 0.01$ are summarized in Table 1. The number of independent runs and the total number of Monte Carlo steps for $h_4 = 2$ and 5 are the same as those used for $h_4 = 1$ at the corresponding system sizes. Similarly, the simulation parameters for $h_4 = 0.001, 0.005, 0.05, 0.1$, and 0.5 are identical to those used for $h_4 = 0.01$. The temperature points are chosen to concentrate around the phase transition regions or near the peaks of the relevant physical quantities, ensuring accurate determination of critical behavior. The first half of the total Monte Carlo steps is discarded to allow the system to reach equilibrium.

Table 1
Summary of the Monte Carlo simulation parameters. L denotes the linear system size, N_r the number of independent runs, N_{MC} the total Monte Carlo steps, N_T the number of temperature points.

	L	N_r	N_{MC}	N_T
$h_4 = 1$	16	5	10.10^6	46
	24	5	10.10^6	46
	32	5	10.10^6	46
	48	5	10.10^6	46
	64	5	10.10^6	41
	96	5	10.10^6	41
	128	5	10.10^6	32
	192	5	10.10^6	25
	256	5	15.10^6	23
$h_4 = 0.01$	16	10	10.10^6	79
	24	10	10.10^6	79
	32	10	10.10^6	79
	48	10	10.10^6	79
	64	10	10.10^6	79
	96	10	10.10^6	68
	128	10	10.10^6	65
	192	10	10.10^6	44
	256	10	15.10^6	41
	384	10	15.10^6	12
	512	10	20.10^6	12

Equilibrium is checked by comparing the specific heat computed from the energy fluctuations with that obtained from the temperature derivative of the energy. Physical quantities are collected after the system has reached equilibrium, with thermal averages computed over the latter half of the Monte Carlo steps. The final estimates are obtained by averaging over several independent simulation runs. The error bars are evaluated using the jackknife method applied to these independent runs.

We measure several physical quantities, including specific heat C, magnetization m, susceptibility χ, Binder ratio g, temperature derivative of Binder ratio dg/dT, correlation length ratio ξ/L, and Z_4-symmetric magnetization m_4.

The specific heat is defined as [6]

$$C = \frac{1}{NT^2}(\langle E^2\rangle - \langle E\rangle^2), \tag{5}$$

where $E =< H >$ is the total energy and N is the number of spins.

The susceptibility is defined as [6]

$$\chi = \frac{N}{T}(\langle m^2\rangle - \langle m\rangle^2), \tag{6}$$

where magnetization $m = m(\vec{0})$ and $m^2 = m(\vec{0})^2$ as defined in Eq. (10).

The Binder ratio is defined as [6,7,13–15]:

$$g = 2 - \frac{\langle m^4\rangle}{\langle m^2\rangle^2}, \tag{7}$$

where $m^2 = m(\vec{0})^2$ and $m^4 = m(\vec{0})^4$. For second-order phase transitions, the Binder ratio typically exhibits a crossing behavior at the critical temperature, where curves corresponding to different system sizes intersect. However, in KT phase transitions, the Binder ratio instead exhibits a merging behavior in KT phase transitions, where the curves for different system sizes converge rather than cross. This merging behavior complicates the precise determination of the critical temperatures. To estimate the critical point more accurately, we compute the temperature derivative of the Binder ratio (dg/dT).

$$\frac{dg}{dT} = \frac{1}{T^2}(-\frac{\langle m^4 H\rangle}{\langle m^2\rangle^2} + \frac{2\langle m^4\rangle\langle m^2 H\rangle}{\langle m^2\rangle^3} - \frac{\langle m^4\rangle\langle H\rangle}{\langle m^2\rangle^2}). \tag{8}$$

The second-moment correlation length is defined as [15–17]

$$\xi = \frac{1}{2sin(k_m/2)}\sqrt{\frac{\langle m(\vec{0})^2\rangle}{\langle m(\vec{k_m})^2\rangle} - 1}, \tag{9}$$

whereas $k_m = (2\pi/L, 0)$. The k-dependent magnetization is expressed as

$$m(\vec{k})^2 = \sum_{\mu=x,y} |\frac{1}{N}\sum_{i=1}^{N} S_{i\mu} exp(i\vec{k}.\vec{r})|^2 \tag{10}$$

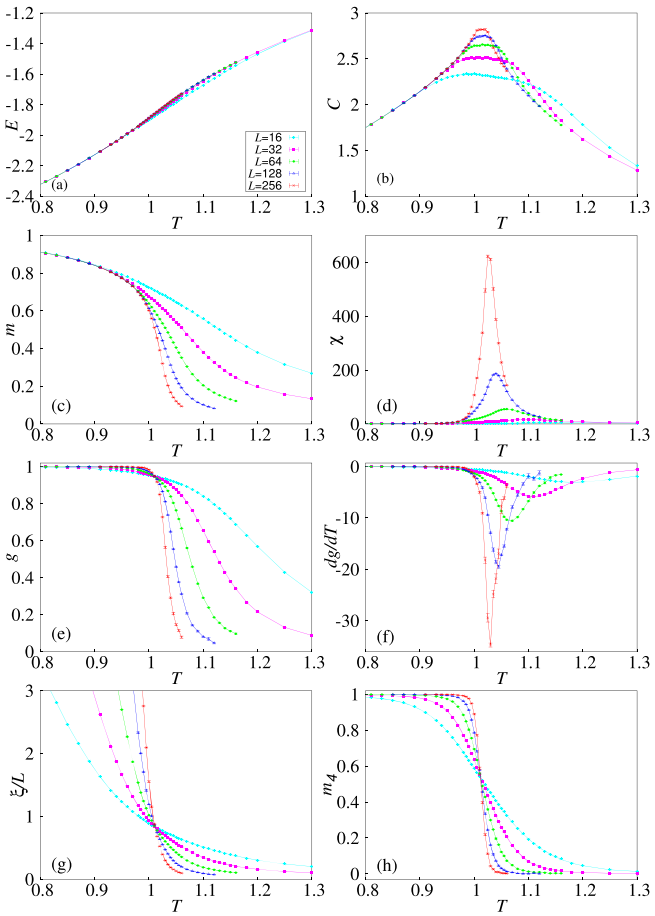

Fig. 1. Temperature and size dependence of energy (a), specific heat (b), magnetization (c), susceptibility (d), Binder ratio (e), temperature derivative of Binder ratio (f), correlation length ratio (g), and Z_4-symmetric magnetization (h) for $h_4 = 1$. Error bars are smaller than the symbol size.

The projections of the spin at site i on the x-axis and y-axis are given by $S_{ix} = \cos\theta_i$ and $S_{iy} = \sin\theta_i$, respectively. The correlation length ratio ξ/L is a useful quantity for characterizing different phases. As the system size L increases, ξ/L diverges to ∞ in the long-range ordered phases, decreases to zero in the disordered phase, and remains finite value in the quasi-long-range ordered phase.

The Z_4 symmetric magnetization is defined as [10,11,18]

$$m_4 = < \cos(4\phi) >, \tag{11}$$

where ϕ denotes the orientation of the global magnetization vector $\vec{m}$. The quantity m_4 has a finite value when ϕ is locked in discrete angles $n\frac{2\pi}{4}$, but vanishes when the angles are uniformly distributed.

3. Simulated results

3.1. Strong anisotropy

Fig. 1 presents the temperature dependence of several physical quantities, including energy (a), specific heat (b), magnetization (c), susceptibility (d), Binder ratio (e), temperature derivative of Binder ratio (f), correlation length ratio (g), and Z_4-symmetric magnetization (h) for $h_4 = 1$. The energy E varies continuously throughout the transition region but exhibits a change in slope near $T \approx 1.01$. Specific heat C exhibits cusp-shaped peaks that sharpen with increasing system size L, consistent with previous studies [12]. For $h_4 = 2$ and 5, C becomes more size-dependent and tends toward a logarithmic divergence similar to that of the four-state clock model. In the strong-anisotropy regime, this behavior agrees with previous results for the XYh_4 model in the triangular lattice [7] and the four-state clock model in the square lattice [19,20], indicating a second-order phase transition. Magnetization m continuously decreases from a finite value at low temperatures to zero near $T \approx 1.01$, indicative of second-order phase transitions. The susceptibility χ also exhibits a single peak that grows with system size. These results resemble previous studies of the XYh_4 model in a triangular lattice [6].

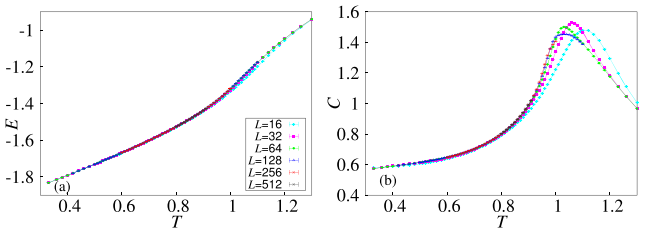

Fig. 2. Temperature and size dependence of the energy (a) and the specific heat (b) for $h_4 = 0.01$. Error bars are smaller than the symbol size.

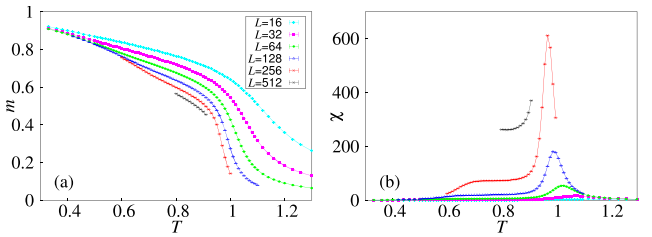

Fig. 3. Temperature and size dependence of the magnetization (a) and the susceptibility (b) for $h_4 = 0.01$. Error bars are smaller than the symbol size.

Binder ratio g curves for different system sizes intersect at a single point. This crossing behavior further supports the presence of a continuous phase transition. The temperature derivative of the Binder ratio shows a sharp divergent peak near $T_c = 1.01$, characteristic of a continuous transition with a finite correlation length exponent ν. From the dip temperature $T_c(L)$ of dg/dT for each system size L, and fitting using Eq. (12) and performing a χ^2-analysis, we obtain $T_c = 1.013 \pm 0.001$ and $\nu = 1.228 \pm 0.025$ for $h_4 = 1$.

$$T_c(L) = T_c + aL^{-1/\nu} \tag{12}$$

The correlation length ratio ξ/L for different sizes also crosses near $T \approx 1.01$. This behavior is consistent with a specific case of the 2D XYh_4h_8 model [12] and similar to that observed in the 2D Ising and 2D four-state clock models [20,21], further confirming a second-order phase transition. From the crossing temperature $T_c(L)$ for each pair of system sizes L and $2L$, and fitting using Eq. (12) and performing a χ^2-analysis, we obtain $T_c = 1.01$ and $\nu = 1.17$ for $h_4 = 1$. We also perform a scaling collapse of ξ/L, using the scaling form $\xi/L = f(tL^{1/\nu})$, where f is the scaling function and $t = T/T_c - 1$ is the reduced temperature. This analysis yields a $Tc = 1.01$ and $\nu = 1.22$. A similar scaling collapse figure for $h_4 = 1$ was presented in our previous work [12]. These values are consistent with the estimates obtained from the analysis of dg/dT, as well as with previous estimates from the analysis of m [5,7].

The Z_4-symmetric magnetization m_4 also shows a distinct crossing near $T_c \approx 1.01$, consistent with estimates from dg/dT, ξ/L. Below T_c, m_4 increases with system size, while above T_c, it vanishes. This indicates that for $h_4 = 1$, the four-fold anisotropy strongly influences the critical behavior.

We note that the present analysis differs substantially from our previous work [12]. While our earlier study of the XYh_4h_8 model focused on the interplay between h_4 and h_8 anisotropies, the case $h_4 = 1$, $h_8 = 0$ was included primarily as a reference point for understanding how the additional h_8 field modifies the nature of the phase transition. In contrast, the present work is specifically devoted to resolving the long-standing question of whether the XYh_4 model with weak anisotropy exhibits a KT transition or a second-order phase transition. Here, the strong-anisotropy case, $h_4 = 1$, is included mainly as a reference point for comparison with the weak-anisotropy regime.

3.2. Weak anisotropy

Fig. 2 shows the temperature dependence of energy (a) and specific heat (b) for $h_4 = 0.01$. The energy varies smoothly across the entire temperature range without exhibiting any singularity or discontinuity. The specific heat C exhibits a size-independent rounded peak at $T \approx 1.0$ for $h_4 = 0.01$ and other weak h_4. This behavior is characteristic of the pure XY model undergoing a KT transition and suggests KT-like behavior in finite systems for weak anisotropy. This contrasts with the expectation of RG that any finite h_4 should suppress the KT transition and lead to a single continuous transition.

Fig. 3 shows the temperature dependence of magnetization (a) and susceptibility (b) for $h_4 = 0.01$. Magnetization m exhibits three distinct behaviors in the temperature range. It is nearly size-independent at low temperatures $T < 0.5$ (ferromagnetic phase), shows a different size dependence at intermediate temperatures $0.5 < T < 0.9$ (suggestive of a KT phase) and vanishes at high temperatures $T > 0.9$ (paramagnetic phase). This behavior is similar to that reported for the XYh_6 model, where the existence of a KT phase has been confirmed by both MC simulations and RG analysis [6,7]. The susceptibility exhibits a peak near $T \approx 0.95$ and a shoulder around $T \approx 0.7$, with the latter expected to develop into a peak for larger L. The presence of these two features suggests the possibility of two phase transitions for $h_4 = 0.01$, consistent with previous numerical studies of the XYh_4 model in a triangular lattice [7] and the XYh_6

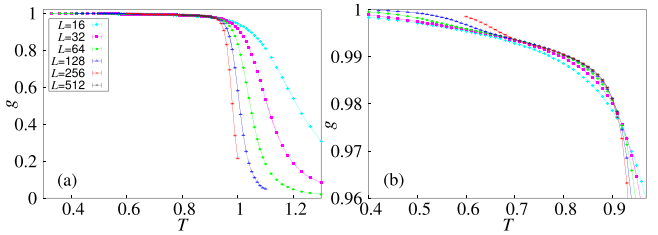

Fig. 4. Temperature and size dependence of the Binder ratio g (a) and zoomed-out view of g (b) for $h_4 = 0.01$. Error bars are smaller than the symbol size.

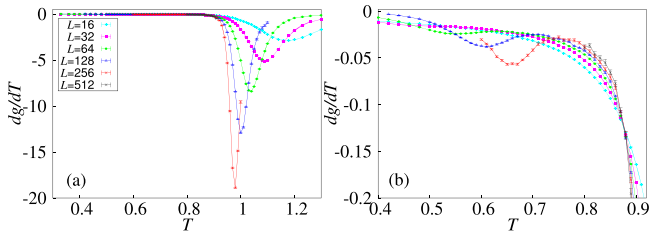

Fig. 5. Temperature and size dependence of the temperature derivative of Binder ratio dg/dT (a) and zoomed-out view of dg/dT (b) for $h_4 = 0.01$. Error bars are smaller than the symbol size.

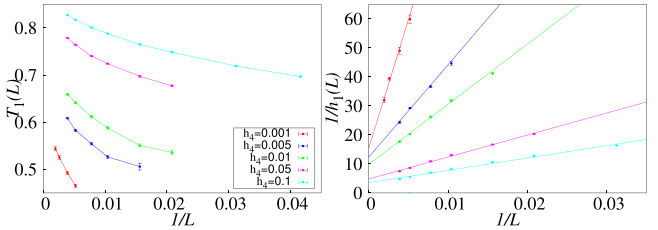

Fig. 6. The dip temperatures of dg/dT versus $1/L$ (a) and invert of depth $1/h_1(L)$ versus $1/L$ (b).

model in a square lattice [6]. However, as seen in Fig. 3(b), it is difficult to determine whether the shoulder temperature corresponds to a true phase transition, so we further analyze other quantities to clarify the nature of this feature.

Fig. 4 shows the temperature dependence of the Binder ratio (a) and its zoomed-out view (b) for $h_4 = 0.01$. As L increases, the Binder ratio g approaches 1 in the low-temperature region ($T < 0.7$) and decreases toward 0 in the high-temperature region ($T > 0.93$). In the intermediate range ($0.7 < T < 0.9$), the g curves for different L tend to merge rather than cross, in contrast to the single crossing observed for strong h_4. This merging behavior is often interpreted as a finite-size signature of a KT phase and has been reported in other models that exhibit the KT phase, such as the 2D TIAFF model [22] and the 2D dimer model [23]. Rastelli et al. also analyzed $g(L)/g(L') \approx 1$ as evidence for KT phase behavior in XYh_4 at intermediate temperatures for weak h_4 [7]. Venus et al. also claimed that XYh_4 exhibits finite-size KT transition [24]. Here, the merging of $g(L)$ suggests $g(L) = g(L')$, implying two distinct KT-like transitions for $h_4 = 0.01$. However, the merging points of g for size pairs (48, 96), (64, 128), (96, 192), and (128, 256) occur approximately 0.63, 0.66, 0.685, and 0.7, respectively, and shift to higher temperatures as L increases.

To probe the critical behavior in the thermodynamic limit, we examined the temperature derivative of the Binder ratio, dg/dT, shown in Fig. 5. dg/dT exhibits two negative dips at $T_1(L)$ and $T_2(L)$, with $T_1(L)$ shifting to higher temperatures and $T_2(L)$ to lower temperatures as L increases.

To analyze the nature of the lower dip in the derivative temperature of the Binder ratio, $T_1(L)$, we attempted to fit its scaling behavior using both KT and second-order transition forms for $h_4 = 0.01$ and other weak value h_4. The KT scaling relation, $T_{KT}(L) = T_{KT} + c^2 T_{KT}/(\ln bL)^2$, proved to be highly unstable. The fits are extremely sensitive to initial seeds and fitting ranges, failing to converge to a unique value. Similarly, a second-order power-law fit, using Eq. (12), failed to provide a consistent description yielding in a T_1 estimate that exceeded the corresponding T_2 value obtained from higher-temperature dip. These instabilities indicate that $T_1(L)$ is not a signature of a true thermodynamic phase transition. Furthermore, analysis of the inverse depth $1/h_1(L)$ as a function of $1/L$ reveals a linear trend for $h_4 = 0.01$ and other weak values h_4 [Fig. 6(b)]. Based on the scaling relation $dg/dT|_{T_1(L)} \sim L^{1/\nu}$, this indicates that ν remains finite, a hallmark of second-order transitions. In addition, $h_1(L)$ does not diverge as $L \to \infty$, indicating that $T_1(L)$ does not correspond to a true phase transition. These results show that the 2D XYh_4 model does not exhibit a KT transition in the thermodynamic limit. Instead, finite-size effects and slow crossovers can produce KT-like features in systems with weak anisotropy, explaining the behavior observed in susceptibility and in previous simulations [7].

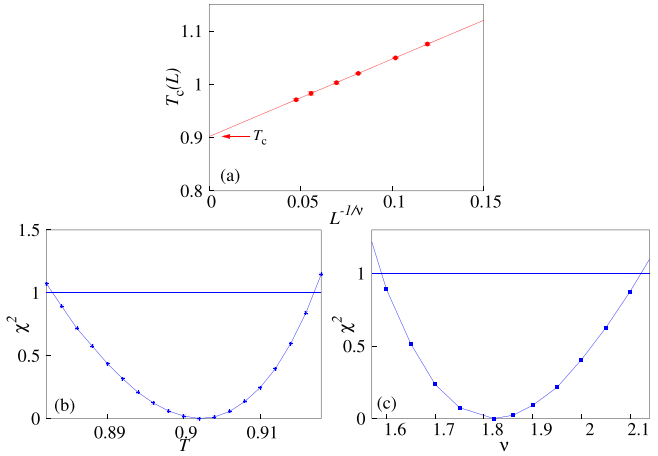

Fig. 7. The fitting and χ^2-analysis of dip temperature $T_2(L)$ of dg/dT using Eq. (12) yield estimate of $T_c = 0.902 \pm 0.020$ and $\nu = 1.82 \pm 0.29$ for $h_4 = 0.01$.

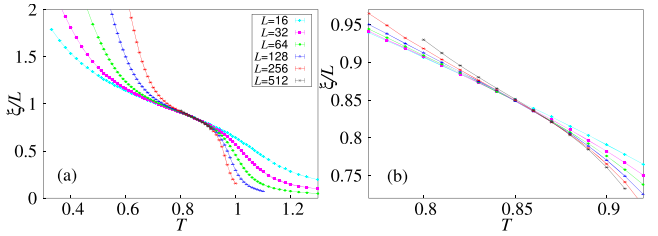

Fig. 8. Temperature and size dependence of the correlation length ξ/L (a) and zoomed-out view of ξ/L (b) for $h_4 = 0.01$. Error bars are smaller than the symbol size.

From the dip temperature $T_2(L)$ of dg/dT for different system sizes L, fitting with Eq. (12), and performing a χ^2-analysis in Fig. 7, we obtain $T_c = 0.902 \pm 0.020$ and $\nu = 1.82 \pm 0.29$ for $h_4 = 0.01$.

Fig. 8 presents the temperature dependence of the correlation length ratio ξ/L in panel (a), along with a zoomed-out view in panel (b), for $h_4 = 0.01$. While other observables in finite systems display KT-like features, the ξ/L curves gradually increase at low temperatures ($T < 0.75$) and decrease towards zero at high temperatures ($T > 0.9$). In the intermediate range ($0.75 < T < 0.9$), the curves ξ/L seem to merge, a behavior typically associated with KT phases and consistent with other observations. However, a closer analysis of each pair of system sizes reveals distinct crossing points that shift slightly toward higher temperatures as L increases. Specifically, the crossing points of ξ/L for the size pairs $(16, 32)$, $(32, 64)$, $(64, 128)$, $(128, 256)$, and $(256, 512)$ occur at approximately 0.822, 0.840, 0.853, 0.862, and 0.867, respectively. These crossings exhibit a systematic trend and appear to converge toward a transition point in the thermodynamic limit, strongly indicating a second-order phase transition at $h_4 = 0.01$.

From the crossing temperature $T_c(L)$ of ξ/L for pair of system sizes L and $2L$, fitting with Eq. (12), and performing a χ^2-analysis in Fig. 9, we obtain $T_c = 0.878 \pm 0.013$ and $\nu = 1.66 \pm 0.75$ for $h_4 = 0.01$. The discrepancy between the crossing temperatures obtained from ξ/L and those extracted from the dip temperatures of dg/dT reflects strong finite-size effects in the weak-anisotropy regime. In this regime, ξ/L exhibits a slow crossover from KT-like behavior at small system sizes to second-order behavior at larger length scales. As a result, the crossing points of ξ/L are not sharply defined and show shift with the system size, leading to significant uncertainty in the critical temperature and exponent. Moreover, similar crossing behavior is observed for other weak anisotropy values $h_4 = 0.001, 0.005, 0.05$, indicating that the XYh_4 model undergoes a second-order phase transition even in the weak anisotropy regime. This finding contrasts with the behavior of the Binder ratio in finite-size KT transitions at weak h_4. The distinct crossing points and scaling behavior of ξ/L in our results therefore provide compelling evidence against KT-type criticality and instead support a second-order transition with non-universal exponents. The scaling collapse of ξ/L for $h_4 = 0.01$ is less satisfactory and does not yield a unique universal curve within the present range of system sizes. We attribute this lack of scaling to the marginal relevance of the four-fold anisotropy. At these length scales, the system is still undergoing a crossover from a $O(2)$-like (where ξ/L curves tend to merge) toward a Z_4-dominated (where distinct crossings emerge).

Fig. 10 shows the temperature dependence of the Z_4-symmetric magnetization m_4 in panel (a) and a zoomed-out view in panel (b) for $h_4 = 0.01$. The m_4 curves for different system sizes L exhibit cross behavior, with the crossing points shifting slightly above T_c toward T_c as L increases. For $T > T_c$, m_4 decreases toward zero, while for $T < T_c$, m_4 increases significantly with increasing L. This behavior is similar to that observed in the 3D XYh_4 model, which undergoes a second-order phase transition [10,25]. Furthermore, the values of $m_4(L)$ (Fig. 10(a)) exceed those of $m(L)$ (Fig. 3(a)) at low temperatures. The crossover temperature $T^*(L)$ shifts upward

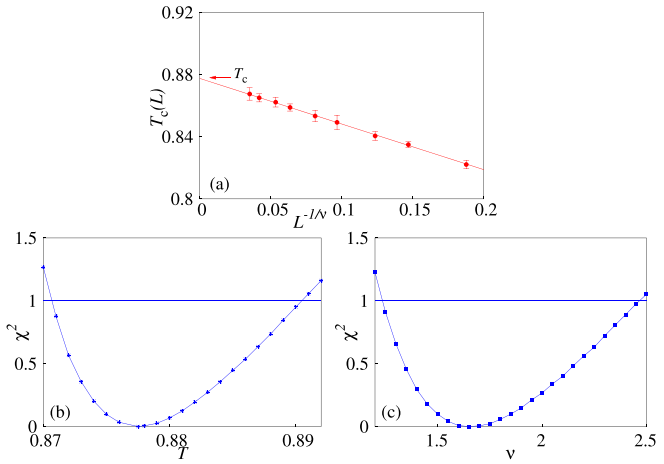

Fig. 9. The fitting and χ^2-analysis of crossing temperature $T_c(L)$ of ξ/L using Eq. (12) yield estimate of $T_c = 0.878 \pm 0.013$ and $\nu = 1.66 \pm 0.75$ for $h_4 = 0.01$.

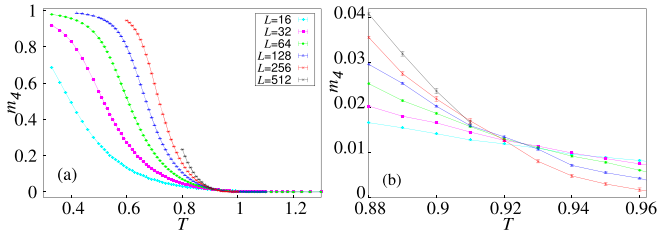

Fig. 10. Temperature and size dependence of the Z_4-symmetric magnetization m_4 (a) and zoomed-out view of m_4 (b) for $h_4 = 0.01$. Error bars are smaller than the symbol size.

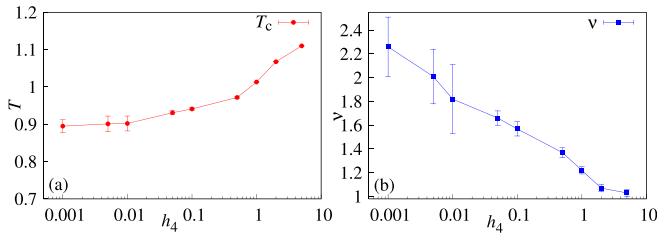

Fig. 11. The critical temperature (T_c) (a) and critical exponent ν (b) as a function of the four-fold anisotropy (h_4) of XYh_4 model.

with increasing L, from $T \approx 0.343$ for $L = 32$, to $T \approx 0.51$ for $L = 64$, to $T \approx 0.613$ for $L = 128$, and to $T \approx 0.685$ for $L = 256$. This behavior is consistent with the prediction of RG that the four-fold anisotropy h_4 acts as a marginally relevant perturbation [1,10]. At small length scales, the effective strength of h_4 is weak, and the system effectively samples the continuous $O(2)$ symmetry of the XY model. However, as the system is coarse-grained to larger scales L, the anisotropy grows under RG flow, and the discrete symmetry Z_4 becomes increasingly dominant. This defines a characteristic length scale $L^*(T)$ at which the system becomes sensitive to the symmetry-breaking field. For $L > L^*$, the spins become increasingly locked into the four preferred directions, causing m_4 to dominate over the continuous magnetization m. The emergence of discrete dominance at larger L is also consistent with the observed crossing behavior of ξ/L, indicating a crossover from $O(2)$-like behavior toward a discrete Z_4 universality class.

3.3. Phase diagram

Fig. 11(a) presents the phase diagram of $T - h_4$ for $h_4 = 0.001, 0.005, 0.01, 0.05, 0.1, 0.5, 1, 2,$ and 5. The critical temperature T_c is determined from the dip temperature $T_2(L)$ of dg/dT for each value h_4. For $h_4 \geq 0.1$, T_c increases with increasing h_4, reflecting that the anisotropy becomes strong enough to dominate over the exchange interaction between neighboring spins. This is consistent with previous numerical results [1,5,7]. For $0.001 \leq h_4 \leq 0.1$, T_c tend to approach the values of $T_{KT} = 0.893$ in the pure XY model as $h_4 \to 0$, suggesting a competition between the intrinsic XY behavior and weak anisotropy.

Fig. 11(b) shows the phase diagram of ν as a function of h_4 for the same set of anisotropy values. The critical exponent ν is obtained from analysis of the dip temperature $T_2(L)$ of dg/dT. For $h_4 \geq 0.5$, ν is found to scale approximately linearly with $1/h_4$, in agreement with previous studies [1,5]. For $h_4 < 0.5$, ν remains finite, which supports a second-order phase transition rather than a KT transition.

The interplay between vorticity and four-fold anisotropy in the 2D XY model leads to a competition that prevents immediate recovery of Ising-like scaling for weak h_4. Instead, the anisotropy acts as a marginal perturbation, generating a line of fixed points that emerges from the vortex-free KT point. Along this line, commonly associated with the Ashkin–Teller universality class, the system exhibits continuously varying (non-universal) critical properties [26]. From this perspective, the variation of ν observed in our results can be interpreted as reflecting the position of the system along this critical line. Consequently, our results for ν provide qualitative support for an Ashkin–Teller–like scenario in the XYh_4 model.

The continuous evolution of ν with h_4 can be related to the experimentally observed "universal window," where effective critical exponents lie between the Ising and XY limits, as discussed in previous work via the "weak universality hypothesis". However, we emphasize that our estimates of ν, obtained from the dip temperatures $T_2(L)$ of dg/dT, are still affected by strong finite-size effects in the weak-anisotropy regime. A more definitive characterization of the dependence of ν on h_4 (e.g., possible logarithmic behavior) would require simulations in significantly larger system sizes. Moreover, since the critical exponent β is not determined in the present study, we cannot examine ratios β/ν to test the "weak universality hypothesis". Therefore, while our results are qualitatively consistent with the "universal window", they are not sufficient to establish it quantitatively.

4. Discussion

Our Monte Carlo simulations shed light on the nature of the phase transition in the 2D XYh_4 model, addressing the long-standing tension between theoretical predictions and numerical results. The key outcome is that, although finite-size effects for weak four-fold anisotropy (e.g., $h_4 \leq 0.1$) may resemble KT-like behavior [6,7], the system ultimately exhibits a second-order phase transition in the thermodynamic limit across the entire range of h_4 studied.

For strong anisotropy ($h_4 > 0.1$), the transition clearly belongs to the second-order universality class, with critical exponents approaching those of the 2D Ising model. This is supported by the diverging specific heat and susceptibility peaks and the characteristic single crossing of the Binder ratio, correlation length ratio curves.

The regime of weak anisotropy ($h_4 \leq 0.1$) is more subtle. Previous Monte Carlo work identified a "bubble of KT phase" for weak h_4 [6,7], where quantities like specific heat and magnetization exhibit features akin to those seen in pure XY models near a KT transition (e.g., rounded, size-independent specific heat peaks) [6,7]. This apparent KT-like region was attributed to finite-size effects or slow crossover dynamics [24]. Our finite-size results for specific heat, magnetization, susceptibility, and Binder ratio align with these observations. However, a deeper analysis of critical behavior in the thermodynamic limit contradicts the KT scenario. The temperature derivative of the Binder ratio reveals a two-peak structure for weak h_4, the low-temperature peak remains finite (suggesting $\nu = \infty$ as in KT), but the divergent high-temperature peak signals a continuous second-order transition. Furthermore, the correlation length ratio and Z_4 symmetric magnetization, even at the smallest h_4, exhibit scaling consistent with second-order behavior rather than the exponential divergence and quasi-long-range order expected for KT. Our numerical results suggest that KT-like features observed at weak h_4 arise from finite-size effects or slow crossovers. In the thermodynamic limit, the transition is second-order, consistent with renormalization group predictions of non-universal exponents for XYh_4 [1].

5. Conclusions

We performed extensive Monte Carlo simulations of the two-dimensional XY model with four-fold anisotropy (XYh_4) to investigate its critical behavior in a wide range of anisotropy strengths (h_4). For large values of h_4 ($h_4 > 0.1$), our results consistently demonstrate a second-order phase transition. The critical exponent ν approaches the 2D Ising value of 1 as $h_4 \to \infty$. For weak h_4 ($h_4 \leq 0.1$), where some previous studies have suggested the presence of a KT phase in both finite and infinite systems, our detailed finite-size scaling analysis points to a different conclusion. Although finite-size systems may exhibit complex features, such as multiple peaks in the temperature derivative of the Binder ratio, our data show that the low-temperature peak does not diverge, and with increasing system size, these peaks tend to merge into a single, diverging high-temperature peak. This, combined with the consistent second-order scaling behavior of the correlation length ratio, strongly supports the conclusion that the 2D XYh_4 model undergoes a second-order phase transition for weak finite h_4 in the thermodynamic limit, with non-universal, continuously varying critical exponents. The KT-like features observed at weak h_4 are most likely finite-size effects or slow crossovers. These effects cause the system to appear XY-like at finite length scales, before the underlying second-order transition with non-universal exponents becomes dominant. Future work should focus on understanding the crossover scaling behavior in the weak h_4 regime more quantitatively to bridge the gap between theoretical predictions and experimental observations of the "universal window" for critical exponents.

CRediT authorship contribution statement

Truong Thi Bach Yen: Writing – original draft, Conceptualization; **Le Thi Thao Vien:** Formal analysis; **Nguyen Tri Tuan:** Visualization; **Dinh Manh Tien:** Resources; **Nguyen Duc Dung:** Validation; **Hoang Mai Anh:** Investigation; **Tran Truong Giang:** Data curation; **Nguyen Vo Nguyen Huy:** Methodology; **Le Chi Luan:** Software; **Duong Xuan Nui:** Writing – review & editing; **Dao Xuan Viet:** Supervision.

Data availability

Data will be made available on request.

Declaration of competing interest

The authors declare that they have no known competing financial interests or personal relationships that could have appeared to influence the work reported in this paper.

Acknowledgments

This research was funded by the Ministry of Education and Training under Grant No. B2023-BKA-19. Numerical calculations were performed using workstations at the School of Materials Science and Engineering, Hanoi University of Science and Technology.

References

[1] J.V. José, L.P. Kadanoff, S. Kirkpatrick, D.R. Nelson, Renormalization, vortices, and symmetry-breaking perturbations in the two-dimensional planar model, Phys. Rev. B 16 (1977) 1217–1241. https://doi.org/10.1103/PhysRevB.16.1217
[2] S. Elitzur, R.B. Pearson, J. Shigemitsu, Phase structure of discrete Abelian spin and gauge systems, Phys. Rev. D 19 (1979) 3698–3714. https://doi.org/10.1103/PhysRevD.19.3698
[3] J.L. Cardy, S. Ostlund, Random symmetry-breaking fields and the XY model, Phys. Rev. B 25 (1982) 6899–6909. https://doi.org/10.1103/PhysRevB.25.6899
[4] S.T. Bramwell, P.C.W. Holdsworth, Magnetization and universal sub-critical behaviour in two-dimensional XY magnets, J. Phys.: Condens. Matter 5 (4) (1993) L53. https://doi.org/10.1088/0953-8984/5/4/004
[5] A. Taroni, S.T. Bramwell, P.C.W. Holdsworth, Universal window for two-dimensional critical exponents, J. Phys.: Condens. Matter 20 (27) (2008) 275233. https://doi.org/10.1088/0953-8984/20/27/275233
[6] E. Rastelli, S. Regina, A. Tassi, Monte Carlo simulation of a planar rotator model with symmetry-breaking fields, Phys. Rev. B 69 (2004) 174407. https://doi.org/10.1103/PhysRevB.69.174407
[7] E. Rastelli, S. Regina, A. Tassi, Monte Carlo simulation for square planar model with a small fourfold symmetry-breaking field, Phys. Rev. B 70 (2004) 174447. https://doi.org/10.1103/PhysRevB.70.174447
[8] U. Wolff, Collective Monte Carlo updating for spin systems, Phys. Rev. Lett. 62 (1989) 361. https://doi.org/10.1103/PhysRevLett.62.361
[9] T. Ala-Nissila, E. Granato, K. Kankaala, J.M. Kosterlitz, S.-C. Ying, Numerical studies of the two-dimensional XY model with symmetry-breaking fields, Phys. Rev. B 50 (1994) 12692–12701. https://doi.org/10.1103/PhysRevB.50.12692
[10] J. Lou, A.W. Sandvik, L. Balents, Emergence of U(1) symmetry in the 3D XY model with Z_q anisotropy, Phys. Rev. Lett. 99 (2007) 207203. https://doi.org/10.1103/PhysRevLett.99.207203
[11] S. Pujari, F. Alet, K. Damle, Transitions to valence-bond solid order in a honeycomb lattice antiferromagnet, Phys. Rev. B 91 (2015) 104411. https://doi.org/10.1103/PhysRevB.91.104411
[12] T.T.B. Yen, D.X. Nui, L.T.N. Tu, N.T. Tuan, N.D. Dung, D.X. Viet, Critical properties in the two-dimensional XY model with four-fold and eight-fold crystal fields, Results Phys. 78 (2025) 108474. https://doi.org/10.1016/j.rinp.2025.108474
[13] D. Loison, Binder's cumulant for the Kosterlitz–Thouless transition, J. Phys.: Condens. Matter 11 (1999) L401. https://doi.org/10.1088/0953-8984/11/34/101
[14] M. Hasenbusch, The Binder cumulant at the Kosterlitz–Thouless transition, J. Stat. Mech. 2008 (2008) P08003. https://doi.org/10.1088/1742-5468/2008/08/P08003
[15] D.X. Viet, H. Kawamura, Monte Carlo studies of chiral and spin ordering of the three-dimensional Heisenberg spin glass, Phys. Rev. B 80 (2009) 064418. https://doi.org/10.1103/PhysRevB.80.064418
[16] Y. Komura, Y. Okabe, Large-scale Monte Carlo simulation of two-dimensional classical XY model using multiple GPUs, J. Phys. Soc. Jpn 81 (11) (2012) 113001. https://journals.jps.jp/doi/10.1143/JPSJ.81.113001.
[17] C. Ding, W. Guo, Y. Deng, Reentrance of Berezinskii-Kosterlitz-Thouless-like transitions in a three-state potts antiferromagnetic thin film, Phys. Rev. B 90 (2014) 134420. https://doi.org/10.1103/PhysRevB.90.134420
[18] S.K. Baek, P. Minnhagen, Non-Kosterlitz-Thouless transitions for the q-state clock models, Phys. Rev. E 82 (2010) 031102. https://doi.org/10.1103/PhysRevE.82.031102
[19] J. Tobochnik, Properties of the q-state clock model for q = 4, 5, and 6, Phys. Rev. B 26 (1982) 6201. https://doi.org/10.1103/PhysRevB.26.6201
[20] L.M. Tuan, T.T. Long, D.X. Nui, P.T. Minh, N.D.T. Kien, D.X. Viet, Binder ratio in the two-dimensional q-state clock model, Phys. Rev. E 106 (2022) 034138. https://doi.org/10.1103/PhysRevE.106.034138
[21] T. Surungan, S. Masuda, Y. Komura, Y. Okabe, Berezinskii–Kosterlitz–Thouless transition on regular and Villain types of q-state clock models, J. Phys. A: Math. Theor. 52 (27) (2019) 275002. https://doi.org/10.1088/1751-8121/ab226d
[22] M. Nishino, S. Miyashita, Termination of the Berezinskii-Kosterlitz-Thouless phase with a new critical universality in spin-crossover systems, Phys. Rev. B 92 (2015) 184404. https://doi.org/10.1103/PhysRevB.92.184404
[23] F. Alet, Y. Ikhlef, J.L. Jacobsen, G. Misguich, V. Pasquier, Classical dimers with aligning interactions on the square lattice, Phys. Rev. E 74 (2006) 041124. https://doi.org/10.1103/PhysRevE.74.041124
[24] D. Venus, Renormalization group analysis of the finite two-dimensional XY model with fourfold anisotropy: application to the magnetic susceptibility of a ferromagnetic ultrathin film, Phys. Rev. B 105 (2022) 235440. https://doi.org/10.1103/PhysRevB.105.235440
[25] P. Patil, H. Shao, A.W. Sandvik, Unconventional U(1) to Z_q crossover in quantum and classical q-state clock models, Phys. Rev. B 103 (2021) 054418. https://doi.org/10.1103/PhysRevB.103.054418
[26] K. Ramola, K. Damle, D. Dhar, Columnar order and Ashkin-Teller criticality in mixtures of hard squares and dimers, Phys. Rev. Lett. 114 (2015) 190601. https://doi.org/10.1103/PhysRevLett.114.190601